DARU Volume 13, No. 3, 2005

MOLECULAR MODELLING OF HUMAN ALDEHYDE OXIDASE AND IDENTIFICATION OF THE KEY INTERACTIONS IN THE ENZYME-SUBSTRATE COMPLEX

SIAVOUSH DASTMALCHI, MARYAM HAMZEH-MIVEHROD

Department of Medicinal Chemistry, School of Pharmacy and Biotechnology Research Centre, Tabriz University of Medical Sciences, Tabriz, Iran.

ABSTRACT

Aldehyde oxidase (EC 1.2.3.1), a cytosolic enzyme containing FAD, molybdenum and iron-sulphur cluster, is a member of non-cytochrome P-450 enzymes called molybdenum hydroxylases which is involved in the metabolism of a wide range of endogenous compounds and many drug substances. Drug metabolism is one of the important characteristics which influences many aspects of a therapeutic agent such as routes of administration, drug interaction and toxicity and therefore, characterisation of the key interactions between enzymes and substrates is very important from drug development point of view. The aim of this study was to generate a three-dimensional model of human aldehyde oxidase (AO) in order to assist us to identify the mode of interaction between enzyme and a set of phethalazine/quinazoline derivatives. Both sequence-based (BLAST) and inverse protein fold recognition methods (THREADER) were used to identify the crystal structure of bovine xanthine dehydrogenase (pdb code of 1FO4) as the suitable template for comparative modelling of human AO. Model structure was generated by aligning and then threading the sequence of human AO onto the template structure, incorporating the associated cofactors, and molecular dynamics simulations and energy minimization using GROMACS program. Different criteria which were measured by the PROCHECK, QPACK, VERIFY-3D were indicative of a proper fold for the predicted structural model of human AO. For example, 97.9 percentages of phi and psi angles were in the favoured and most favoured regions in the ramachandran plot, and all residues in the model are assigned environmentally positive compatibility scores. Further evaluation on the model quality was performed by investigation of AO-mediated oxidation of a set of phthalazine/quinazoline derivatives to develop QSAR model capable of describing the extent of the oxidation. Substrates were aligned by docking onto the active site of the enzyme using GOLD technology and then HASL method were used to generate a 3D-QSAR model. Correlation coefficient (r^2) between the test set actual and predicted K_m values was 0.65.

Keywords: Aldehyde oxidase, Molecular modeling, 3D-QSAR, genetic algorithm.

INTRODUCTION

Molybdenum hydroxylases are non-CYP450 enzymes capable of catalysing the oxidation of drugs. This group of hydroxylases, which includes aldehyde oxidase (aldehyde:oxygen oxidoreductase, EC 1.2.3.1; AO), xanthine oxidase (EC 1.1.3.22; XO) and xanthine dehydrogenase (EC 1.1.1.204; XDH) are more commonly found in the cytosol of mammalian liver, and carry out the oxidation and detoxification of a number of structurally different azaheterocycles. These proteins are characterized by the presence of a molybdoptrin cofactor which is essential for the catalytic activity and generally oxidises the carbon α to the nitrogen of the azaheterocycle to oxo metabolites, also called lactams. They catalyse their reactions differently than CYP450 and other hydroxylase enzymes requiring water rather than molecular oxygen as the source of the oxygen atom incorporated into the metabolite according to the following formula (1):

$$RH + H_2O \rightarrow ROH + 2\bar{e} + 2H^+$$

where RH and ROH are the substrate and the hydroxylated metabolite respectively. From the structural point of view, human aldehyde oxidase is a large dimeric protein with a molecular weight of approximately 300 kDa, composed of two identical subunits (150 kDa). Each subunit contains two non-identical 2Fe/2S redox centers, a flavin adenin dinucleotide (FAD) and a molybdoptrin binding site (2). It can oxidize a wide range of substrates including aldehydes and N-heterocyclic compounds such as purine, pyrimidine (3), quinoline (4), quinazoline, phtalazine (5), pyridine (4) and their derivatives.

Aldehyde oxidase is widely distributed throughout the animal kingdom, such as rat, bovine (6), rabbit (3,6), baboon, guinea pig (7) and monkey (8). Two

Correspondence: Siavoush Dastmalchi, Department of Medicinal Chemistry, School of Pharmacy, Tabriz Univerity of Medical Sciences, Tabriz, Iran, Email: dastmalchi.s@tbzmed.ac.ir

isoenzymes of aldehyde oxidase have been identified in potato tubers. Aldehyde oxidase is also found to be prevalent amongst molluscs, crustaceans and insects (6).

Aldehyde oxidase is found in the liver, kidney, lung, spleen, stomach, muscle and heart. Of all the mammalian tissues, the liver contains the highest level of aldehyde oxidase and other organs such as the lung, kidney and small intestine containing less than 50% of hepatic enzyme activity (6).

As to the significance of aldehyde oxidase in pathological conditions, the protein is involved in the mechanism of ethanol generated hepatotoxicity and may be of importance in the generation of some of the symptoms observed in the rare heredity disease known as "combined deficiency of molybdenum proteins". More recently, genetic evidence has implicated aldehyde oxidase in the genesis of the familial recessive form of amyotrophic lateral sclerosis (ALS), a rare and severe motor neuron disease characterized by progressive muscular paralysis leading to death. In this type of hereditary pathological state, the candidate gene maps on chromosome 2q33-q35, a very short distance from a genetic marker co-segregating with the disease.

Molybdenum is the only second-row transition metal that is required by most living organisms (9). Because of its unique chemical versatility and unusually high bioavailability, which is useful to biological system, this metal has been incorporated into the active site of enzymes over the course of evolution (9).

Aldehyde oxidase is known to metabolise endogenous compounds like retinaldehyde (2,10), pyridoxal ($VitB_6$) (6), N-methyl nicotinamide (6,8), dihydroxymandelaldehyde (2), endogeous purines (6) and benzaldehyde (8).

In addition to the endogenic role for AO, this enzyme plays an important role in the biotransformation of xenobiotics such as famciclovir (11), methotrexate (12,13), azathioprine (5), quinine (5,14), quinidine (5), carbazeran (5,6), allopurinol (5,15), zaleplon (16,17), brimonidine (18), *o*-benzylguanine (6,19,20) , zonisamide (1,8), MPTP(1-methyl-4-phenyl-1,2,3,6-tetrahydropyridine) (21), 5-fluoro-2-pyrimidine (a prodrug) (22) deoxyguanine (23), s-nicotine (24,25), ziprasidone (26,27), sulindac, imipiramin N-oxide (8), thioguanine (1), N-(2-(dimethylamino) ethyl] acridine – 4 - carboxamide (DACA) (1,14) and other compounds.

The important inhibitors of aldehyde oxidase which can influence the metabolism of drugs, are cimetidine (17) , raloxifene (28) , menadione (1,11) , methadone (29), SKF-252A (30), hydralazine (31), isovanillin (11), β-stradiol (32), disulfiram, chloralhydrate, glyceraldehydes (33), potassium cyanide (1), promethazine, chlorpromazine, amobarbital, dihydroxy progestron, quinacrine, diphenylhydramine, dicumarol and etc (34).

It would be useful to know the mechanism by which aldehyde oxidase carries out its function in atomic level. Therefore, an understanding of the manner of the interactions of aldehyde oxidase with its substrates would be useful in designing of efficient substrates or potent inhibitors for this enzyme which can influence enzyme activity. The function of a protein is generally determined by its three dimensional structure. However, there is no report on the 3D-strucure of human aldehyde oxidase empirically. In the present study, comparative protein structure modelling and 3D-QSAR methods were used to determine 3D-structure of this enzyme and to analyse the interactions between the enzyme and its substrates. The biochemical function of a protein is defined by its interactions with other molecules and the biological function is a consequence of these interactions. Functional characterisation of a protein sequence is one of the most frequent problems in biology. This task is usually facilitated by accurate three-dimensional (3D) structure of under study protein. In the absence of an experimentally determined structure, comparative or homology modelling can sometimes provide a useful 3D model for a protein of the unknown structure (the target), which can be built based on one or more related proteins of known structures (the templates).

MATERIALS AND METHODS

All structure coordinates for the proteins which were used in this study were retrieved from the Protein Data Bank at the Research Collaboratory for Structural Bioinformatics (35) (http://www.RCSB.org). The BLAST (version 2.2.9) search engine, which is publicly available at National Centre for Biotechnology Information (NCBI) (http://www.ncbi.nlm.nih.gov/BLAST/) was used to find the homologous proteins with known structures to be used as the template in comparative modelling of AO (36). For the alignment between sequences of AO and few homologous proteins, CLUSTALW was used from its web site at http://www2.ebi.ac.uk/CLUSTALW (37). Among them bovine xanthine dehydrogenase (pdb code of 1FO4) has known structure and is used as the template for model building (38). There was 49.8% identity between sequences of AO and bovine xanthine dehydrogenase (XDH).

THREADER program (version 3.4) was used as the inverse-folding method of fold recognition (39). Calculations were performed on a silicon graphics O2 workstation (IRIX 5.6 system). The

results were evaluated based on the z-score which is calculated to accommodate the sum of pairwise pseudo-energy potentials as well as residue solvation. A THREADER database file for XDH structure was prepared and added to the THREADER fold library (~.tdb).

The Swiss pdb Viewer program for windows (Deepview version 3.7) was downloaded from ExPASY proteomics server of the Swiss Institute of Bioinformatics (http://www.expasy.ch/spdbv/) and used as a viewing program as well as performing the modelling job. Deepview was used to thread the sequence of AO onto the structure of template (XDH) based on the alignment proposed by CLUSTAL W and to submit the modelling job to the SWISS-MODEL server:
(http://www.expasy.org/swissmod/
SWISSMODEL.HTML) (40). The initial rough model from SWISS-MODEL was superimposed with the template structure to add cofactors to the model (Fe/S, FAD, MO-Pt). Side chain conformations were further adjusted to eliminate steric clashes and unfavoured geometries.

Modelled protein structure was energy minimised using GROMACS program (version 3.1.1) while positioned in a box of water molecules ($123.5\times123.5\times123.5$ $Å^3$) under conjugate gradient and periodic boundary conditions (41,42). The structure file for the ensemble consists of protein main chain, cofactors and the substrate in the appropriate format recognisable to GROMACS program was prepared using pdb2gmx command of GROMACS package and PRODRG server at http://davapc1.bioch.dundee.ac.uk/programs/
prodrg/prodrg.html (43). Gaussian molecular orbital program implemented in the HyperChem package was used to calculate the charges for the atoms of the cofactor and substrate molecules. The calculated charges were used to edit the topology files generated by the PRODRG server.

Molecular dynamics simulation was carried out after 25 ps of water equilibration where the non-water components were fixed. During the simulation for every 1.000 ps the actual frame was stored.

The energy minimized average structure calculated from the equilibrated trajectory system was evaluated for quality of protein geometry and structure folding reliability. Subsequently, the dynamic behaviour and structural changes of the protein was analysed by calculation of a commonly used parameter indicating the structure movement is the root mean square deviation (RMSD).

The quality of protein geometry was checked employing PROCHECK (version 3.5.4) (44,45). The output of PROCHECK is a series of files wich evaluates different aspects of the model's quality. One of the most important outputs (evaluations) is the Ramachandran plot, which allows pointing out those residues with anomalous combinations of φ and ψ angles. Other model evaluation methods are Verify-3D (46,47), used from its web server (http://www.doe-mbi.ucla.edu/Verify3d.html) and QPACK program (version 1.1) (48).

3D structures of the substrates (tables 1 and 2) were generated using the Hyperchem (version 5.0) model built option. The initial structures were first minimised using molecular mechanics MM+ force field (49). Then, those structures were fully optimised based on the semiemperical MNDO method, available in Hyperchem (50). The output structures (*.hin) were converted to SYBYL Cartesian coordinate files (*.mol2) using BABEL program (version 1.6) in order to be used as an acceptable format in GOLD (version 2.0) and AutoDock (version 3.0.5) programs with the aim of docking (51,52). The coordinate of molybdenum (Mo) atom was used as the centre of the active site of the enzyme. Flexible docking of all compounds under the investigation was carried out using GOLD program running on Windows XP. Docking was performed by applying a distance constraint of 2.5-3.5Å between atom from substrate known to be involved in the oxidation (atom which will be oxidised) and Mo atom from the protein. Early termination was allowed if the top three solutions were within 1.5 Å RMSD. GoldScore was selected for scoring function, and the population size, number of operations and number of islands were set to 100, 100,000 and 5 respectively. GOLD parameter file was edited to include parameters such as atom type, van der Waals radius, ionisation potential and polarizability for Mo atom. The alignments were achieved among the compounds based on the docking performed by GOLD were used for 3D-QSAR studies as outlined below. AutoDock was used on an O2 sgi workstation according to the User's Guide documentation of the program (52).

The HASL method (version 3.30) was used for the purpose of generating 3D-QSAR model using the ligands aligned according to the docking procedure outlined above (53-55). The substrates were randomly divided into the training and test groups consist of 22 and 7 compounds, respectively. The training and test set which were chosen in this study are indicated in tables 1 and 2. Training set of substrates were used to generate a

3D-QSAR model in order to predict the biological activity (log k_m) of the test set at resolution values of 2, 3 and 4 Å.

RESULTS

Three-dimensional model of human aldehyde oxidase

Human aldehyde oxidase (AO) structure was modelled using the crystal structure of bovine xanthine dehydrogenase (XDH) as the template for comparative modelling. The initial model was built via replacement of the sequence of AO with that of the structure of XDH guided by the multiple alignment generated using the sequences of AO, XDH and few homologous proteins, namely aldehyde oxidase from bovine, rabbit and rat as well as the sequence of chicken XDH as shown in Table 1. Total of six loops were built during the process of generating the initial model at Swiss-Model sever. The size of the loops ranged from 4 to 8 residues including the anchoring residues except for that of the region between LYS^{166} and SER^{198}, which consists of two helical segments. This initial model which is free from cofactors and substrate molecules was energy minimised using GROMOS 43B1 force field at the server. To the model which was obtained from Swiss-Model server was added the cofactor molecules, MOS, FAD, Fe/S and MTE in the positions assumed from their corresponding locations in the crystal structure of XDH. The model was inserted into a box of SPC water molecules (56) and energy minimised prior to molecular dynamics simulation (Figure 1). Plot of the potential energy against time (Figure 2. panel A) for the ensemble of model structure in water during unconstrained molecular dynamics simulation shows that the energetically stable model was obtained in about 20 ps. In the same time, the RMSD differences for the C^{α} atoms of model plus heavy atoms of MTE (phosphonic acid mono-(2-amino-5,6-dimercapto-4-oxo-3,7,8A,9,10,10A-hexahydro-4H-8-oxa-1,3,9,10-tetraaza antracen-7-yl methyl) ester), MOS, and substrate (P7 in Table 2) molecules reaches a plateau (Figure 2 panel B) indicating the stability of the model. The conformational changes of the model structure of AO during the MD simulation were also evaluated by analysing the RMSD values between pairs of structures sampled at different elapsed times. The results given in Table 4 shows that the RMSD values range between 1.17 to 1.82 Å. Results in Table 5 shows that the content of secondary structure elements of the model which was calculated on the basis of the DSSP algorithm (57) remains constant during the MD simulation.

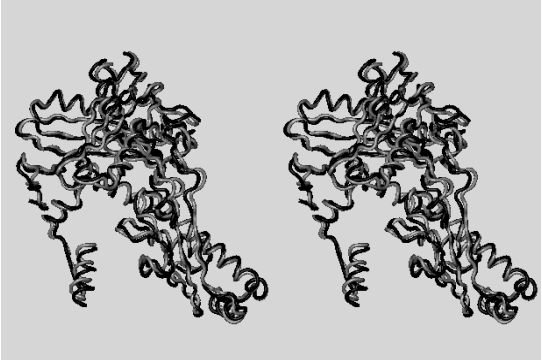

Figure 1. Tube representation of the model of human aldehyde oxidase (shown in gray) superimposed with the template structure of bovine xanthine dehydrogenase (pdb code of 1FO4, shown in black). For clarity, only the parts of the model and the structure corresponding to the residues indicated in the alignment presented in Table 1 are shown. The RMSD value for the shown superimposition is 1.29 Å.

Quality assessment of the model

The quality of the model was evaluated using following means. Ramachandran plot shows that more than 97.9% of the φ/ψ angles of the residues are located in the favoured and most favoured regions (Figure 3). According to PROCHECK the optimised model shows relatively good protein geometry, and most of the quality parameters being better than average or in the range of tolerance (thresholds). Although no clashes between residues of the model have been identified by DeepView, there were total of 41 marginally bad contacts between atoms of the minimised model listed by PROCHECK. The distances between the contacting atoms ranged from 2.3 to 2.6 Å and all of them were removed upon MD simulation.

The reliability of protein folding appears to be good because the secondary structures are stable during molecular dynamics simulation (Table 4) and the RMSD deviation between the starting model and the model after 60 ps free MD simulation is 1.67Å which is less than the resolution (2.1 Å) at which the template structure has been solved by X-ray crystallography.

The third domain of AO (Mo-Pt domain) was uploaded to Verify-3D server (46,47) to analyse the compatibility of the residues with their environment in the model. The result obtained is shown in figure 4. As it can be seen from the figure there is no residue with the negative compatibility score, which indicates the proper fold for the model. The result from Verify-3D is in agreement with the result obtained from THREADER (39), another inverse protein folding method. The z-score calculated by THREADER for threading the sequence of AO onto the structure of XDH was 5.69 which is well above

Table 1. Part of the sequence alignment used for building homology model of human aldehyde oxidase (target sequence) based on the structure of bovine xanthine dehydrogenase (template structure). Because of the space limitation the sequences for the other homologous proteins used in the multiple alignment were not shown.

Sequence name	Sequence alignment	Residue number
ADO_HUMAN	AAVTAFAANKHGRAVRCVLERGEDMLITGGRHPYLGKYKAGFMNDGRILALDMEHYSNAG	877
XDH_BOVIN	SVAVALAAYKTGHPVRCMLDRNEDMLITGGRHPFLARYKVGFMKTGTIVALEVDHYSNAG	867
	:...*:** * *:.***:*:*.**********:*.:**.***: * *:**:::******	
SS Element	HTHHHHHHHHHSS EEEE HHHHHHHS B EEEEEEEEEE TTS B EEEEEEEE B	
ADO_HUMAN	ASLDESLFVIEMGLLKMDNAYKFPNLRCRGWACRTNLPSNTAFRGFGFPQAVLITESCIT	937
XDH_BOVIN	NSRDLSHSIMERALFHMDNCYKIPNIRGTGRLCKTNLSSNTAFRGFGGPQALFIAENWMS	927
	* * * ::* .*::***.**:**:* * *:***.********* ***::*:*. ::	
SS Element	SS TTHHHHHHHHHHTTTTTB SEEEEEEEEEE SS TTTTHHHHHHHHHHHHH	
ADO_HUMAN	EVAAKCGLSPEKVRIINMYKEIDQTPYKQEINAKNLIQCWRECMAMSSYSLRKVAVEKFN	997
XDH_BOVIN	EVAVTCGLPAEEVRWKNMYKEGDLTHFNQRLEGFSVPRCWDECLKSSQYYARKSEVDKFN	987
	....*:** ***** * * ::*.::. .: :** **: *.* ** *:***	
SS Element	HHHHHHT HHHHHHHHB TT B TT B S HHHHHHHHHHHHTTHHHHHHHHHHHH	
ADO_HUMAN	AENYWKKKGLAMVPLKFPVGLASRAAGQAAALVHIYLDGSVLVTHGGIEMGQGVHTKMIQ	1057
XDH_BOVIN	KENCWKKRGLCIIPTKFGISFTVPFLNQAGALIHVYTDGSVLVSHGGTEMGQGLHTKMVQ	1047
	** ***:**.::* ** :.:: .**.**:*:* ******:*** *****:****:*	
SS Element	HH SSEEEEEEEEEEEEES SSGGG EEEEEEEE TTS EEEEES SSS HHHHHHH	
ADO_HUMAN	VVSRELRMPMSNVHLRGTSTETVPNANISGGSVVADLNGLAVKDACQTLLKRLEPIISKN	1117
XDH_BOVIN	VASKALKIPISKIYISETSTNTVPNSSPTAASVSTDIYGQAVYEACQTILKRLEPFKKKN	1107
	.: *::*:*:::: ***:****:. :..** :*: * ** :****:******: .**	
SS Element	HHHHHHTS GGGEEE EETTTS S S TT HHHHHHHHHHHHHHHHHHHHHTHHHHT	
ADO_HUMAN	PKGTWKDWAQTAFDESINLSAVGYFRGYESDMNWEKGEGQPFEYFVYGAACSEVEIDCLT	1177
XDH_BOVIN	PDGSWEDWVMAAYQDRVSLSTTGFYRTPNLGYSFETNSGNAFHYFTYGVACSEVEIDCLT	1167
	.:*:**. :*::: :.**:.*::* : . .:*...*:.*.**.**.**********	
SS Element	TT HHHHHHHHHHTT EEEEEEE SS BTTTTBS S SEEEEEEEEEEEEETTT	
ADO_HUMAN	GDHKNIRTDIVMDVGCSINPAIDIGQIEGAFIQGMGLYTIEELNYSPQGILHTRGPD	1234
XDH_BOVIN	GDHKNLRTDIVMDVGSSLNPAIDIGQVEGAFVQGLGLFTLEELHYSPEGSLHTRGPS	1224
	*****:*********.*:********:****:**:**:*:***:***:* ******.	
SS Element	EEE EEEEEEE BS S TTHHHHTHHHHHHHHHHHHHT B TTS B STT	

[a]SS indicates the secondary structure elements quoted in the protein structure database for the crystal structure of template (XDH) and the followings are the definitions of different SS elements: H=helix; B=residue in isolated beta bridge; E=extended beta strand; G=310 helix; T=hydrogen bonded turn; S=bend. ADO_HUMAN and XDH_BOVIN are human aldehyde oxidase (SWISS-PROT AN: Q06278) and bovine xanthine dehydrogenase (SWISS-PROT AN: P80457) sequences respectively. " * "," : " and "." represent identical, conserved and semi-conserved substitutions, respectively.

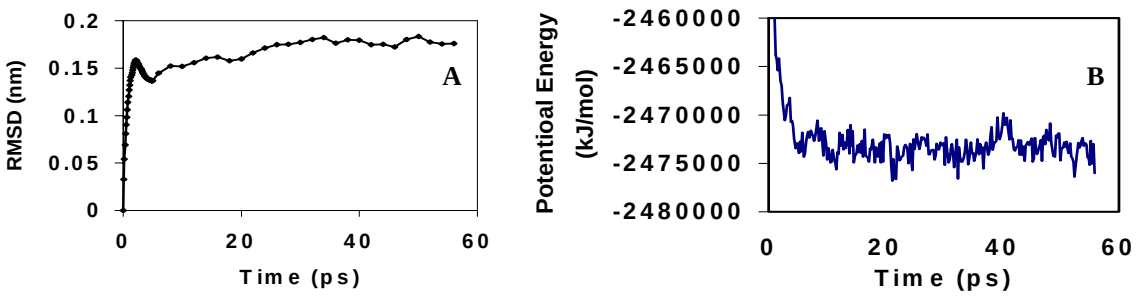

Figure 2. C^{α} root mean square deviation (RMSD) of the model structure of human aldehyde oxidase (Panel A) and the variation of the potential energy of the model (Panel B) during the molecular simulation.

Table 2. Phthalazine derivatives used in 3D-QSAR model and the corresponding K_m (μM).

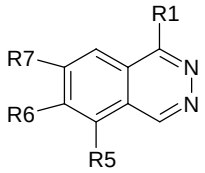

Phthalazine No.	R1	R5	R6	R7	K_m(μM) [c]
P1 [a]	H	H	H	H	41
P2 [a]	Cl	H	H	H	9
P3 [b]	Cl	H	$-OCH_3$	$-OCH_3$	30
P4 [a]	$-OC_2H_5$	H	H	H	43
P5 [a]	$-C_6H_5$	H	H	H	9
P6 [a]	$-OC_6H_5$	H	H	H	150
P7 [b]		H	H	H	39
P8 [a]	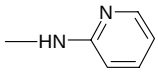	H	H	H	35
P9 [a]	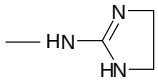	H	H	H	26
P10 [a]	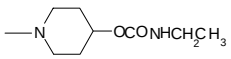	H	$-OCH_3$	$-OCH_3$	52
P11 [a]	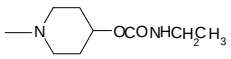	$-OCH_3$	$-OCH_3$	$-OCH_3$	130
P12 [a]	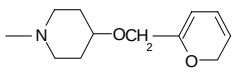	H	$-OCH_3$	$-OCH_3$	23
P13 [a]	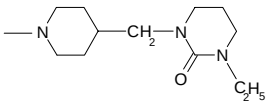	H	$-OCH_3$	$-OCH_3$	220
P14 [b]	$NHCH_2CH_2N(CH_3)_2$	H	H	H	37

[a]Training set, [b]Test set, [c]Data taken from (5).

the z-value required for making correct fold prediction with a high level of confidence (i.e. 3.5).

The packing of the model was evaluated using the QPACK method and results shows that the residues in the model occupy their ideal volumes with an average sphere size equal to 99% ± 14 of the ideal size.

In order to evaluate the quality of the model further, we have used it in a 3D-QSAR study. 3D-QSAR studies rely heavily on the goodness of the alignment generated among the molecules which were used in the study. If the method of the alignment is based on the docking of the molecules onto the binding site of the receptor, the reliability of the alignment and the 3D-QSAR models depend on the quality of the docking algorithm as well as the receptor structure and/or model. We have chosen GOLD and AutoDock methods for docking purposes as these methods are among the best known algorithms available for ligand as well as protein flexible docking (58).

3D-QSAR calculations using HASL method were carried out on the compounds, which were aligned using genetic algorithm implemented in GOLD program. HASL model for 3D-QSAR studies were

achieved by using 22 compounds as a learning set and 7 compounds as a test set, as are indicated in tables 1 and 2. The predictivity of the model was measured as the correlation coefficient (r^2) between test set actual and predicted K_m values. The best r^2 of the prediction of K_m values for the test set compounds was 0.65 (Figure 5), which was achieved by using the lattice resolution of 3 Å and rotational increment of 10 degrees. The HASL model which was generated by using all compounds gave a correlation close to unity. The results of the HASL program on the compounds aligned using AutoDock were not as good as those achieved by GOLD alignment and thus no reports are given in this article.

Table 3. Quinazoline derivatives used in 3D-QSAR model and the corresponding K_m (μM)

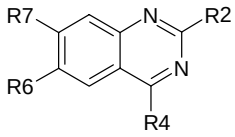

Quinazoline No.	R2	R4	R6	R7	K_m (μM)[c]
Q1 [a]	H	H	H	H	21
Q2 [b]	H	H	NH_2	H	41
Q3 [a]	H	H	NO_2	H	77
Q4 [a]	H	H	H	NH_2	140
Q5 [b]	CH_3	H	H	H	15
Q6 [a]	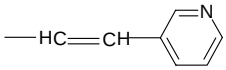	H	H	H	15
Q7 [a]	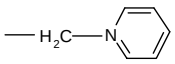	H	H	H	400
Q8 [a]	H	-$CH(CH_2OH)_2$	H	H	300
Q9 [b]	H	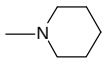	H	H	78
Q10 [a]	H	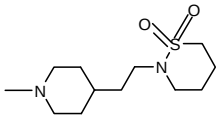	H	H	35
Q11 [a]	H	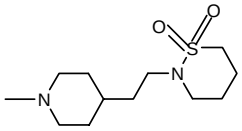	-OCH_3	H	10
Q12 [a]	H	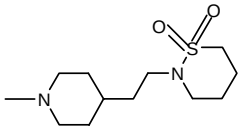	H	-OCH_3	13
Q13 [a]	H	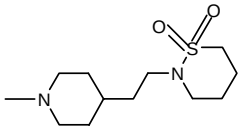	-OCH_3	-OCH_3	33
Q14 [a]	H	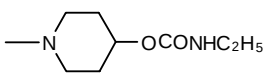	H	H	43
Q15 [b]	H	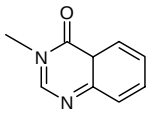	H	H	17

[a]Training set, [b]Test set, [c]Data taken from (5).

The results from docking study using GOLD program indicates specific interactions. These interactions are shown for compound P7 in figure 6. Investigation of the P7-AO complex shown in figure 6 indicates presence of a π-π stacking interaction between benzene ring of the phethalazine core structure and phenyl side chain of Phe^{923}. Nitrogen in position 3 of phethalazine is 1.82 Å away from amide proton of Ala^{1019} in a direction suitable for making a hydrogen bond interaction. Another polar interaction can be identified between Glu^{882} carboxyl group and the terminal hydroxyl group of the hydroxyethyl side chain of the R1 substitution in P7 compound. Residues containingPhe^{655}, Phe^{885}, Leu^{1018} and Ala^{1023} in active site of enzyme create a hydrophobic environment, which interact with the aliphatic regions of pyridine ring and ethyl moiety.

Table 4. RMSD values between pairs of structure of AO during MD simulation at two different elapsed times indicated by Time 1 and Time 2.

Structure at		RMSD (Å)
Time 1 (ps)	Time 2 (ps)	
1	58	1.67
2	30	1.82
4	30	1.51
16	30	1.16
2	4	1.17

Table 5. Percentages of the residues in different classes of secondary structure[a] during last 30 ps of MD simulation of the AO model in water

Secondary structure	Percentages	SD[b]
Structured[c]	62.0	0.7
Coil	22.2	0.5
β-sheet	19.5	0.6
β-bridge	2.0	0.3
Bend	13.7	0.4
Turn	11.7	0.4
α-helix	28.8	0.3
3-helix	2.2	0.3

[a]Secondary structures were assigned using DSSP algorithm (57), [b]Standard deviation
[c]Structured means the sum of percentages of the residues in α-helix, β-sheet, β-bridge and Turn secondary structures.

DISCUSSION

Drug metabolism is one of the important characteristics, which influences many aspects of a therapeutic agent, such as the routes of administration, drug interaction and toxicity. Therefore, the ability to predict the extent of biotransformation via a particular pathway is very important from drug development point of view. Aldehyde oxidase (AO) is involved in the metabolism of wide range of endogenous compounds such as retinaldehyde, pyridoxal, purine and N-methylnicotinamide. However, more important in drug development is the role of AO in the biotransformation of many drug substances such as famciclovir, methotrexate, zaleplon and zonisamide and there are many other compounds used in the therapeutics (e.g. cimetidine, raloxifene and methadone), which can inhibit AO and this can be the source of drug interaction. Therefore, understanding of the way that AO interacts with its substrates in the atomic level would be useful in the design of efficient substrates or potent inhibitors of this enzyme.

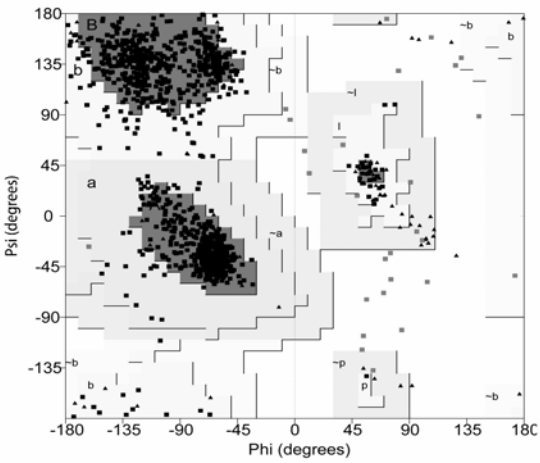

Figure 3. Ramachandran plot of human aldehyde oxidase model. The most favoured regions (A, B, L) are shadowed dark grey (86.9%), the favoured regions (a, b, l, p) are marked medium grey (11.0%), additionally allowed regions (~a, ~b, ~l, ~p) are shadowed in light grey (1.0%). The residue numbers of the non-Gly and non-Pro amino acids located in the disallowed region (1.2%) are 2, 59, 151, 163, 195, 238, 382, 398, 433, 533, 541, 651, 663, 715, 787, 804, 878, 893, 918, 956, 1145, 1198, 1252, 1291, 1323 and 1324.

The aim of this study was to build the structural model of aldehyde oxidase and to develope 3D-QSAR model in order to predict the extent of oxidation of quinazoline and phthalazine classes of compounds by this enzyme. After model construction and structural refinement by molecular dynamics simulation and energy minimization, model evaluation methods indicates that the model structures have good geometry. The distribution of φ/ψ angles (Ramachandran-plot shown in figure 3) is satisfactory with 97.9% of the non-glycine and non-proline residues located

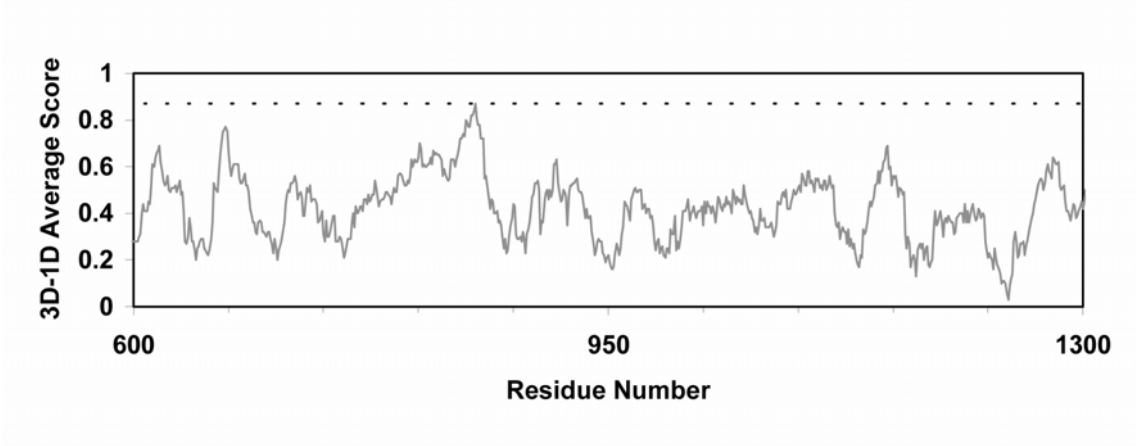

Figure 4. Verified-3D analysis is shown for the residues 600 to 1300, and the positive scores suggest that the residues are compatible with their environments in the model built for human aldehyde oxidase.

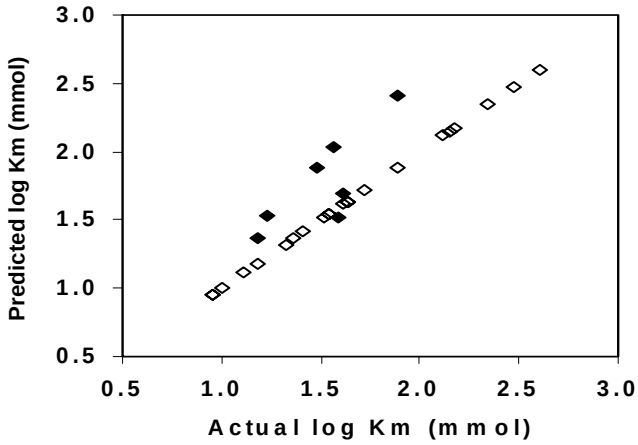

Figure 5. Actual values of log K_m *vs* predicted values of log K_m. The correlation coefficient (r^2) found between test set actual and predicted log K_m values (shown as filled squares, ◆) was 0.65. The open squares (◇) show the actual and predicted log K_m values using all of the compounds.

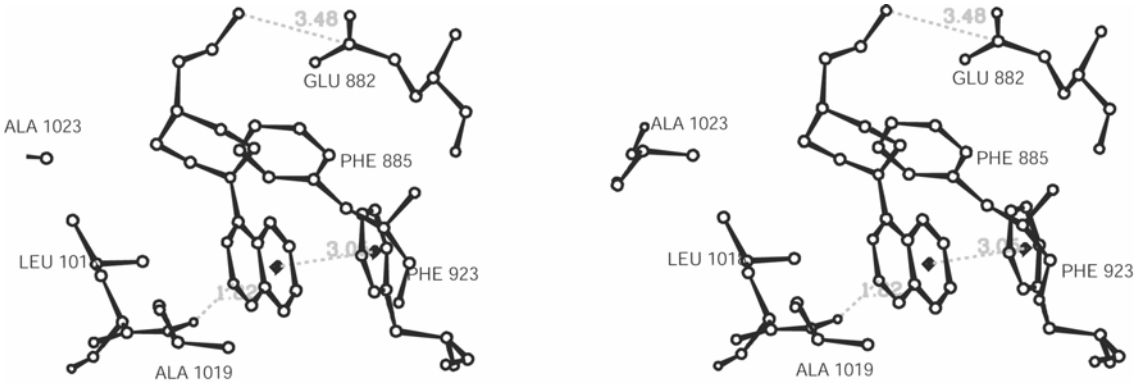

Figure 6. Stereo presentation of the residues interacting with the substrate P7 docked into the active site. Phe^{655} and hydrogen atoms are not shown for clarity except for the amide proton of Ala1019 where a hydrogen bond is formed between enzyme and substrate.

in favoured and most favoured regions. The result of Verified-3D analysis suggest that in the proposed model for AO, residues are compatible with their environment in the model as it is evident from strongly positive 3D-1D scores in Figure 4. Secondary structure content of the model remained constant during MD simulation (Table 4) and the RMSD values between starting model structure of AO and those of different times during the course of MD simulation were small (1.16-1.82Å) in the range which were observed for different structural ensemble determined for a protein by using NMR technique (59).

There are considerable evidences to suggest that binding of both substrates and inhibitors to enzyme are facilitated by hydrophobic interaction in the enzyme active site (6). Simple unsubstituted monocycles such as pyridine, pyrazine, pyrimidine, pyridazine and pyrrole show little or negligible binding to the enzyme. However, it has been shown that fusion or substitution of a phenyl group significantly increases the affinity of the compounds towards AO (6). It has been reported that the increase in lipophilcity of compounds leads to decrease in the K_m values. For example the most lipophilic compound Q11 (Table 3) gave the lowest K_m value (10μM) and other lipophilic compounds (Q6, Q10, Q12 and Q13) also shows high affinity (K_m value <40 μM) (5,7). These findings are in agreement with our results obtained from docking studies. As discussed in previous section, there is a hydrophobic region (Phe^{885}, Phe^{655}, Leu^{1018} and Ala^{1023}) in the active site of enzyme, which is responsible for hydrophobic interaction. It has been pointed out that the orientation of lipophilic regions may also be important for binding of substrates into the active site. For example, fusion of a benzene ring from positions 3 and 4 in quinoline leads to the efficient substrate of 3,4-benzoquinoline, while introduction of benzene ring to other positions produces compounds (5,6- and 7,8-benzoquinolines), which do not bind the enzyme properly (6). In addition to hydrophobic pocket in the active site of enzyme, there is a π-π interaction between the benzene ring fused to the heterocyclic ring of substrate and the side chain of Phe^{923} of enzyme. The distance between geometric centres of the benzene rings involved in this interaction is 3.06 Å as shown in Figure 6. Hydrogen binding interaction is also observed between heterocyclic nitrogen of substrates and amide proton of Ala^{1019}. Another possible hydrogen bond can be formed between hydroxyl group of R1 substituent of P7 and Glu^{882}, in which a hydrogen atom, either from hydroxyl group of substrate or from carboxyl group of residue 882, and three oxygen atoms from these groups may be involved in a three-centred fashion.

In an attempt to provide a meaningful 3D-QSAR model, 22 compounds in the training set were docked onto the active site of the model structure to generate receptor-based alignment. The aligned structures were used to calculate a HASL model. Prediction of the binding constants (log k_m) using the HASL model for the test set of 7 compounds gave an r^2 of 0.65. The substrates used in this study have wide range of substituents and also show a narrow range of k_m values (less than two orders of magnitude) and in addition the flexible nature of the active site which is necessary to make it possible to oxidize structurally broad range of compounds, reduce the prediction capability of the 3D-QSAR studies.

In conclusion, in this study we have built a model for human aldehyde oxidase, which shows appropriate geometry and stability which are verified by different means. The model was used to develop a 3D-QSAR using K_m values for a set of phethalazine/quinazoline derivatives.

ACKNOWLEDGEMENTS

The authors would like to thank Tabriz University of Medical Sciences, Tabriz, Iran for providing the financial support for this work.

REFERENCES

1. Williams DA. Drug metabolism. In: Williams DA, Lemke TL, editors. Foye's principles of medicinal chemistry. 5 ed. Philadelphia: Lippincott Williams and Wilkins; 2002. p 199-200.
2. Terao M, Kurosaki M, Demontis S, Zanotta S, Garattini E. Isolation and characterization of the human aldehyde oxidase gene: conservation of intron/exon boundaries with the xanthine oxidoreductase gene indicates a common origin. Biochem J 1998; 332: 383-93.
3. Hall WW, Krenitsky, T.A. Aldehyde oxidase from rabbit liver: Specificity toward purines and their analogs. Arch Biochem Biophys 1986; 251: 36-46.
4. Krenitsky TA, Neil SM, Elion GB, Hitchings GH. A comparison of the specificities of xanthine oxidase and aldehyde oxidase. Arch Biochem Biophys 1972; 150: 585-99.
5. Ghafourian T, Rashidi MR. Quantitative study of the structural requirments of phtalazine/ quinazoline derivatives for interaction with human liver aldehyde oxidase. Chem Pharm Bull 2001; 49: 1066-71.
6. Beedham C. Molybdenum hydroxylases: Biological distribution and substrate-inhibitor specifity. In: Ellis GP, West GB, editors. Prog Med Chem. Volume 24. Amsterdam: Elseveir; 1987. p 85-127.

7. Beedham C, Critchley DJP, Rance DJ. Substrate specifity of human aldehyde oxidase towards substituted quinazolines and phthalazines: A comparison with hepatic enzyme from guinea pig, rabbit and baboon. Arch Biochem Biophys 1995; 319: 481-90.
8. Kitamura S, Nakatani K, Ohashi K, Sugihara K, Hosokawa R, Akagawa Y, Ohta S. Extremely high Drug-Reductase activity based on Aldehyde oxidase in monkey liver. Biol Pharm Bull 2001; 24: 856-59.
9. Hille R. Molybdenum and tungsten in biology. Trends Biochem Sci 2002; 27: 360-67.
10. Ambroziak W, Izaguirre, G., Pietruszko, R. Metabolism of retinaldehyde and other aldehydes in soluble extracts of human. J Biol Chem 1999; 274: 33366-73.
11. Clarke SE, Harrell, A.W., Chenery, R.J. Role of aldehyde oxidase in the in vitro conversion of famciclovir to penciclovir in human liver. Drug Metab Dispos 1995; 23: 251-54.
12. Jordan CG, Rashidi MR, Laljee H, Clarke SE, Brown JE, Beedham C. Aldehyde oxidase-catalysed oxidation of methotrexate in the liver of guinea-pig, rabbit and man. J Pharm Pharmacol 1999; 51: 411-18.
13. Bannwarth B, Pehourcq F, Schaeverbeke T, Dehais J. Clinical pharmacokinetics of low-dose pulse methotrexate in rheumatoid arthritis. Clin Pharmacokinet 1996; 30: 194-210.
14. Al-salmy HS. Inter-strain variability in aldehyde oxidase activity in the mouse. Comparative biochemistry and Physiology Part C: Toxicology and Pharmacology 2002; 132: 341-47.
15. Moriwaki Y, Yamamoto T, Yamakita J, Takahashi S, Tsutsumi Z, Higashino K. Zonal distribution of allopurinol-oxidizing enzymes in rat liver. Adv Exp Med Biol 1998; 431: 47-50.
16. Cates LA, Jones GSJ, Good DJ, Tsai HY, Li VS, Caron N, Tu SC, Kimball AP. Cyclophosphamide potentiation and aldehyde oxidase inhibition by phosphorylated aldehydes and acetals. J Med Chem 1980; 23: 300-04.
17. Renwick AB, Ball SE, Tredger JM, Price RJ, Walters DG, Kao J, Scatina JA, Lake BG. Inhibition of zaleplon metabolism by cimetidine in the human liver: in vitro studies with subcellular fractions and precision-cut liver. Xenobiotica 2002; 32: 849-62.
18. Acheampong AA, Chein DS, Lam S, Vekich S, Breau A, Usansky J, Harcourt D, Munk SA, Nguyen H, Garst M, Tang-Liu D. Characterization of brimonidine metabolism with rat, rabbit, dog, monkey and human liver fractions and rabbit aldehyde oxidase. Xenobiotica 1996; 26: 1035-55.
19. Roy SK, Korzekwa KR, Gonzalez FJ, Moschel RC, Dolan ME. Human liver oxidative metabolism of O6-benzylguanine. Biochem Pharmacol 1995; 50: 1385-89.
20. Roy SK, Gupta E, Dolan ME. Pharmacokinetics of O6-benzylguanine in rats and its metabolism by rat liver microsomes. Drug Metab Dispos 1995; 23: 1394-99.
21. Yoshihara S, Ohta S. Involvement of hepatic aldehyde oxidase in conversion of 1-methyl-4-phenyl-2,3-dihydropyridinium (MPTP+) to 1-methyl-4-phenyl-5,6-dihydro-2-pyridone. Arch Biochem Biophys 1998; 360: 93-98.
22. Guo X, Lerner-Tung M, Chen HX, Chang CN, Zhu JL, Chang CP, Pizzorno G, Lin TS, Cheng YC. 5-Fluoro-2-pyrimidinone, a liver aldehyde oxidase-activated prodrug of 5-fluorouracil. Biochem Pharmacol 1995; 49: 1111-16.
23. Harrell AW, Wheeler SM, East P, Clarke SE, Chenery RJ. Use of rat and human in vitro systems to assess the effectiveness and enzymology of deoxyguanine analogs as prodrugs of an antiviral agent. Drug Metab Dispos 1994; 22: 189-93.
24. Berkman CE, Park SB, Wrighton SA, Cashman JR. In vitro-in vivo correlations of human (S)-nicotine metabolism. Biochem Pharmacol 1995; 50: 565-70.
25. Cashman JR, Park SB, Yang ZC, Wrighton SA, 3rd. Jp, Benowitz NL. Metabolism of nicotine by human liver microsomes: stereoselective formation of trans-nicotine N$^{'}$-oxide. Chem Res Toxicol 1992; 5: 639-46.
26. Beedham C, Miceli JJ, Obach RS. Ziprasidone metabolism, aldehyde oxidase, and clinical implications. J Psychopharmacol 2003; 23: 229-32.
27. Caley CF, Cooper CK. Ziprasidone: the fifth atypical antipsychotic. Ann Pharmacother 2002; 36: 839-51.
28. Obach RS. Potent inhibition of human liver aldehyde oxidase by raloxifene. Drug Metab Dispos 2004; 32: 89-97.
29. Robertson IG, Gamage RS. Methadone: a potent inhibitor of rat liver aldehyde oxidase. Biochem Pharmacol 1994; 47: 584-87.
30. Robertson IG, Bland TG. Inhibition by SKF-525A of the aldehyde oxidase-mediated metabolism of the experimental antitumor agent acridine carboxamide. Biochem Pharmacol 1993; 45: 2159-62.
31. Johnson C, Stubley-Beedham C, Stell JG. Hydralazine: a potent inhibitor of aldehyde oxidase activity in vitro and in vivo. Biochem Pharmacol 1985; 34: 4251-56.
32. S.M. V, Dachtler SL. Effects of sex hormones on hepatic aldehyde oxidase activity C57BL/6J mice. Horm Res 1981; 14: 250-59.

33. Donelli MG, Bartosek I, A. G, Martini A, Colombo T, Pacciarini MA, Modica R. Importance of pharmacokinetic studies on cyclophosphamide (NSC-26271) in understanding its cytotoxic effect. Cancer Treat Res 1976; 60: 395-401.
34. Zollner H. Handbook of enzyme inhibitors. Weinheim; 1999. 100-01 p.
35. Berman HM, Westbrook J, Feng Z, Gililand G, Bahat TN, Weissig H, Shindyalov PE. The protein data bank. Nucleic Acids Res 2000; 28: 235-42.
36. Altschul SF, Gish W, Miller W, Myers EW, Lipman DJ. Basic Local Alignment Search Tool. J Mol Biol 1990; 215: 403-10.
37. Thompson JD, Higgins DG, Gibson TJ. CLUSTAL W: Improving the sensitivity of progressive multiple sequence alignment through sequence weighting, position-specific gap penalties and weight matrix choice. Nucleic Acids Res 1994; 22: 4673-80.
38. Enroth C, Eger BT, Okamoto K, Nishino T, Pai EF. Crystal structures of bovine milk xanthine dehydrogenase and xanthine oxidase: Structure-based mechanism of conversion. Biochemistry 2000; 97: 10723-28.
39. Jones DT, Miller RT, Thornton JM. Successful protein fold recognition by optimal sequence threading validated by rigorous blind testing. Proteins: Struct, Funct, Genet 1995; 23: 387-97.
40. Guex N, Peitsch MC. SWISS-MODEL and the Swiss pdb viewer: An environment for comparative protein modelling. Electrophoresis 1997; 18: 2714-23.
41. Berendsen HJC, Van der Spoel D, Van Drunen R. GROMACS: A message-passing parallel molecular dynamics implementation. Comput Phys Commun 1995; 91: 43-56.
42. Lindahl E, Hess B, Van der Spoel D. GROMACS 3.0: A package for molecular simulation and trajectory analysis. J Mol Mod 2001; 7: 306-17.
43. Van Aalten DMF, Bywater R, Findlay JBC, Hendlich M, Hooft RWW, Vriend G. PRODRG, a program for generating molecular toplogies and unique molecular descriptors from coordinates of small molecules. J Comput Aided Mol Des 1996; 10: 255-62.
44. Laskowski RA, MacArthur MW, Moss DS, hornton JM. Procheck: A program to check the stereochemical quality of protein structures. J Appl Crystallogr 1993; 26: 283-91.
45. Morris AL, MacArthur MW, Hutchinson EG, Thornton JM. Stereochemical quality of protein structure coordinates. Proteins: Struct, Funct, Genet 1992; 12: 345-64.
46. Bowie JU, Luthy R, Eisenberg D. A method to identify protein sequences that fold into a known three-dimensional structure. Science 1991; 253: 164-70.
47. Luthy R, Bowie JU, Eisenberg D. Assessment of protein models with three-dimensional profiles. Nature 1992; 356: 83-85.
48. Gregoret LM, Cohen FE. A novel method for the rapid evaluation of packing in protein structures. J Mol Biol 1990; 211: 959-74.
49. Allinger NL. Conformational analysis 130. MM2. A hydrocarbon force field utilizing v1 and v2 torsional terms. J Am Chem Soc 1977; 99: 8127-34.
50. Dewar MJS, Thiel W. Grond states of molecules.39.MNDO results for molecules containing hydrogen, carbon, nitrogen and oxygen. J Am Chem Soc 1977; 99: 4907-17.
51. Jones G, Willett P, Glen RC. Molecular recognition of receptor sites using a genetic algorithm with a description of desolvation. J Mol Biol 1995; 245: 43-53.
52. Morris GM, Goodsell DS, Halliday RS, Huey R, Hart WE, Belew RK, Olson AJ. Automated docking using a Lamarckian genetic algorithm and empirical binding free energy function. J Comput Chem 1998; 19: 1639-62.
53. Doweyko AM. The hypothetical active site lattice. An approach to modelling active sites from data on inhibitor molecules. J Med Chem 1988; 31: 1396-406.
54. Doweyko AM, Mattes WB. An application of 3D-QSAR to the analysis of the sequence specifity of DNA alkylation by uracil mustard. Biochemistry 1992; 31: 9388-92.
55. Doweyko AM. Three-Dimensional pharmacophores from binding data. J Med Chem 1994; 37: 1769-78.
56. Ferguson DM. Parametrization and evaluation of a flexible water model. J Comput Chem 1995; 16: 501–11.
57. Kabsch W, Sander C. Dictionary of protein secondary structure: pattern recognition of hydrogen-bonded and geometrical features. Biopolymers 1983; 22: 2577-637.
58. Morris GM, Olson, A.J., Goodsell, D.S. Protein-Ligand docking. In: Clark DE, editor. Evolutionary algorithms in molecular design. Volume 8, Methods and principles in medicinal chemistry. Weinheim: WILLEY-VCH; 2000. p 32-39.
59. Abagyan RA, Totrov MM. Contact area difference (CAD): a robust measure to evaluate accuracy of protein models. J Mol Biol 1997; 268: 678-85.